

# Dynamical dipole $\gamma$ radiation in heavy-ion collisions on the basis of the quantum molecular dynamics model

H. L. Wu,<sup>1,2</sup> W. D. Tian,<sup>1</sup> Y. G. Ma,<sup>1,\*</sup> X. Z. Cai,<sup>1</sup> J. G. Chen,<sup>1</sup> D. Q. Fang,<sup>1</sup> W. Guo,<sup>1</sup> and H. W. Wang<sup>1</sup>

<sup>1</sup>*Shanghai Institute of Applied Physics, Chinese Academy of Sciences, P.O. Box 800-204, Shanghai 201800, China*

<sup>2</sup>*Graduate School of the Chinese Academy of Sciences, Beijing 100080, China*

(Dated: July 11, 2018)

Dynamical dipole  $\gamma$ -ray emission in heavy-ion collisions is explored in the framework of the quantum molecular dynamics model. The studies are focused on systems of  $^{40}\text{Ca}$  bombarding  $^{48}\text{Ca}$  and its isotopes at different incident energies and impact parameters. Yields of  $\gamma$  rays are calculated and the centroid energy and dynamical dipole emission width of the  $\gamma$  spectra are extracted to investigate the properties of  $\gamma$  emission. In addition, sensitivities of dynamical dipole  $\gamma$ -ray emission to the isospin and the symmetry energy coefficient of the equation of state are studied. The results show that detailed study of dynamical dipole  $\gamma$  radiation can provide information on the equation of state and the symmetry energy around the normal nuclear density.

PACS numbers: 25.70.Gh, 24.30.Cz, 25.70.Ef, 25.70.Lm

Giant dipole resonance (GDR)  $\gamma$ -ray emission built on heavy-ion collisions, which was predicted in early macroscopic models [1, 2] has been widely studied both experimentally and theoretically during the past few decades [3, 4]. It can be ascribed to a collective vibration of protons against neutrons with a dipole spatial pattern that starts with the overlap of two nuclei in both fusion or incomplete fusion. Recently, a so-called dynamical dipole mode (pre-equilibrium GDR) that is generated by a high-amplitude dipole collective motion of nucleons before the formation of a fully equilibrated compound nucleus (CN) has been discussed [5–7] and it can encode information about the early stage of collisions when the CN is still in a highly deformed configuration. Some efforts have been made to study the dipole resonance formed during fusion in  $N/Z$  asymmetry heavy-ion reactions as it could be a good probe for the symmetry term in the equation of state (EOS), which is one of the hotly debated issues related to nuclear astrophysics problems such as the elements burning in supernova [8].

Several microscopic transport simulations, such as time-dependent Hartree-Fock [5], Boltzmann-Nordheim-Vlasov [9], and constrained molecular dynamics [10], have been successfully used to study GDR dynamical dipole emission. However, the quantum molecular dynamics (QMD) model, which has been effectively used to dispose problems of heavy-ion collisions up to 2 GeV/nucleon [11], has not been used to investigate GDR. In principle, energy is not conserved in the QMD model and the model is more suited for higher-energy phenomena. But, it is still of interest to see how the QMD model works for GDR  $\gamma$  radiation and discuss its properties.

We use the isospin-dependent QMD (IDQMD) model, which is based on the general QMD model but embodies the isospin degrees of freedom in two-body nucleon-nucleon collisions and Pauli blocking, as well as consid-

ering the difference between neutron and proton density distributions for nuclei far from the  $\beta$ -stability line and treating the sampling of neutrons and protons in the initialization in phase space, respectively [12, 13].

The mean field involved in the present IDQMD model is given by  $U(\rho) = U^{\text{Sky}} + U^{\text{Coul}} + U^{\text{Yuk}} + U^{\text{sym}}$ , with  $U^{\text{Sky}}$ ,  $U^{\text{Coul}}$ ,  $U^{\text{Yuk}}$ , and  $U^{\text{sym}}$  representing the Skyrme potential, the Coulomb potential, the Yukawa potential and the symmetry potential interaction, respectively [11]. The Skyrme potential is  $U^{\text{Sky}} = \alpha(\rho/\rho_0) + \beta(\rho/\rho_0)^\gamma$ , where  $\rho_0 = 0.16 \text{ fm}^{-3}$  (the saturation nuclear density) and  $\rho$  is the nuclear density. We take the parameters  $\alpha = -356 \text{ MeV}$ ,  $\beta = 303 \text{ MeV}$ , and  $\gamma = 7/6$ , corresponding to a soft EOS, and  $\alpha = -124 \text{ MeV}$ ,  $\beta = 70.5 \text{ MeV}$ , and  $\gamma = 2$ , corresponding to a stiff EOS.  $U^{\text{Yuk}}$  is a long-range interaction that is necessary to describe the surface of the nucleus and takes the following form:  $U^{\text{Yuk}} = (V_y/2) \sum_{i \neq j} \exp(Lm^2)/r_{ij} \cdot [\exp(mr_{ij}) \text{erfc}(\sqrt{L}m - r_{ij}/\sqrt{4L}) - \exp(mr_{ij}) \text{erfc}(\sqrt{L}m + r_{ij}/\sqrt{4L})]$  with  $V_y = 0.0024 \text{ GeV}$ ,  $m = 0.83$ , and  $L$  is the so-called Gaussian wave-packet width (here  $L = 2.0 \text{ fm}^2$ ).  $r_{ij}$  is the relative distance. In principle, if one adds  $U^{\text{Yuk}}$  into the effective potential, some part of the two-body term in  $U^{\text{loc}}$  should be subtracted. Therefore  $\alpha$  should be smaller [11]. However, considering that we aim to discuss some qualitative effects of the stiffness of potential on pre-equilibrium GDR  $\gamma$  emission, we tentatively keep the preceding two sets of potential parameters.

In recent years, some efforts have been made to constrain the symmetry energy term of the EOS from nuclear reactions induced by asymmetric heavy ions, and various probes have been proposed [8]. Considering that the pre-equilibrium GDR  $\gamma$  ray originates from the isospin nonequilibrium of the entrance channel or the composite intermediate system, its spectra should be dependent on the symmetry potential. The symmetry potential in the

\*Corresponding author. Email: ygma@sinap.ac.cn

IDQMD model is obtained by

$$U^{\text{sym}} = \frac{C_{\text{sym}}}{2\rho_0} \sum_{i \neq j} \tau_{iz} \tau_{jz} \frac{1}{(4\pi L)^{3/2}} \exp\left[-\frac{(r_i - r_j)^2}{4L}\right] \quad (1)$$

with  $C_{\text{sym}}$  the symmetry energy strength,  $\tau_z$  being the  $z$ th component of the isospin degree of freedom, which equals 1 or  $-1$  for neutrons or protons, respectively. A detailed description of the QMD model is given in Ref.[11].

The giant dipole moment in coordinator space [ $DR(t)$ ] and in momentum space [ $DK(t)$ ] is written, respectively, as follows [14]:

$$DR(t) = \frac{NZ}{A} X(t) = \frac{NZ}{A} (R_Z - R_N), \quad (2)$$

where  $X(t)$  is the distance between the centers of mass of protons and neutrons,  $R_Z = \sum_i x_i(p)$  and  $R_N = \sum_i x_i(n)$  is the center of mass of protons and neutrons, respectively, and

$$DK(t) = \frac{NZ}{A\hbar} \Pi(t) = \frac{NZ}{A\hbar} \left( \frac{P_p}{Z} - \frac{P_n}{N} \right) \quad (3)$$

is just the canonically conjugate momentum of the  $DR(t)$ , where  $\Pi(t)$  denotes the relative momentum, with  $P_n$  ( $P_p$ ) centers of mass in momentum space for neutrons (protons).

Here  $N = N_P + N_T$  and  $Z = Z_P + Z_T$ , the suffix  $P$  (or  $T$ ) marks projectile (or target). We have adopted the initial dipole moment as follows:

$$\begin{aligned} DR(t=0) &= \frac{NZ}{A} |R_Z(t=0) - R_N(t=0)| \\ &= \frac{R_P + R_T}{A} Z_P Z_T \left| \left( \frac{N}{Z} \right)_T - \left( \frac{N}{Z} \right)_P \right|, \end{aligned} \quad (4)$$

where  $R_P$  and  $R_T$  are the radii of the projectile and target, respectively.

Derived from the overall dipole moment  $D(t)$ , we can get the  $\gamma$ -ray emission probability for energy  $E$  [4]

$$\frac{dP}{dE} = \frac{2}{3\pi} \frac{e^2}{E\hbar c} \left| \overline{\frac{dV_k}{dt}}(E) \right|^2, \quad (5)$$

where  $dP/dE$  can be interpreted as the average number of  $\gamma$  rays emitted per energy unit, while  $\overline{\frac{dV_k}{dt}}(E)$  is the Fourier transformation of the time derivative on the  $k$ th components  $x$  and  $z$  of  $\overline{\vec{V}}$ ,

$$\overline{\frac{dV_k}{dt}}(E) = \int_0^\infty \frac{dV_k}{dt}(t) e^{i(Et/\hbar)} dt, \quad (6)$$

where  $\overline{V}$  denotes the dipole resonance of the system and was derived from the total dipole according to the equation

$$\overline{V_k} = \frac{dD(t)_k}{dt}. \quad (7)$$

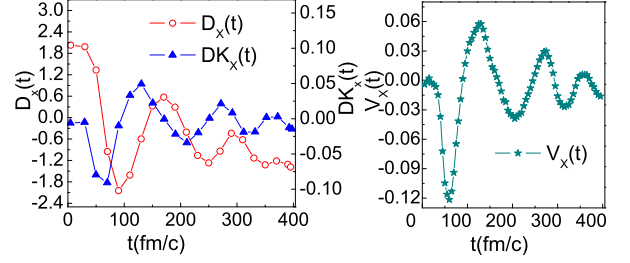


FIG. 1: (Color online) Left: Evolution of the giant dipole moment with time in coordinate space [ $D_x(t)$ ] and momentum space [ $DK_x(t)$ ]. Right: Dynamical dipole mode [ $V_x(t)$ ]. The reaction system is  $^{40}\text{Ca}+^{48}\text{Ca}$  collision at 10 MeV/nucleon with  $b=1$  fm and soft EOS parameters.

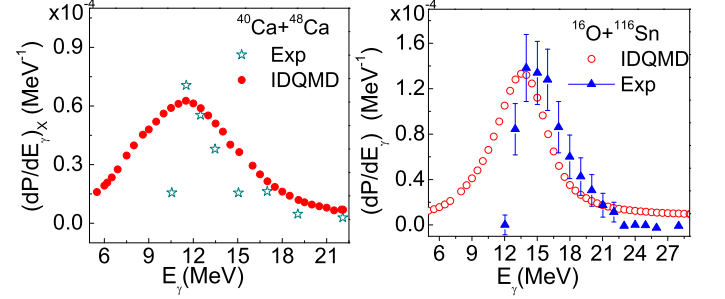


FIG. 2: (Color online) Left: Experimental data (stars) [10] together with our IDQMD model [filled (red) circles] of the  $\gamma$ -ray spectrum of the  $^{40}\text{Ca}+^{48}\text{Ca}$  system at 10 MeV/nucleon. Right: Measured value of  $\gamma$ -ray yield for the  $^{16}\text{O}+^{116}\text{Sn}$  system at 15.6 MeV/nucleon (open circles) [7] and our calculation results [filled (blue) triangles] under the same conditions.

Figure 1 shows the evolution of the giant dipole moment with time in coordinate space and momentum space for  $^{40}\text{Ca} + ^{48}\text{Ca}$  collisions at 10 MeV/nucleon and  $b = 1$  fm. The giant dipole moment attenuates rapidly after  $t = 400$  fm/c, illustrating a clear reduction of the collective behavior. The similar behavior is observed for the pre-equilibrium or dynamical dipole mode [denoted  $V_x(t)$ ].

To determine the reliability of our calculations of dipole emission with the IDQMD model, experimental data for the  $^{40}\text{Ca}+^{48}\text{Ca}$  system [10] at  $E_{\text{beam}} = 10$  MeV/nucleon and the  $^{16}\text{O}+^{116}\text{Sn}$  system [7] at  $E_{\text{beam}} = 15.6$  MeV/nucleon are compared with our results in Fig. 2. It should be noted that the experimental data on dynamical dipole emission here are obtained by taking away the statistical contribution (results of the statistical model) from the measured spectra. In addition, calculations for both systems are carried out with soft Skyrme potential and impact parameters being a triangle distribution between 1 and 6 fm. The good agreement between the data and the IDQMD calculation encourages us to make systematic calculations on pre-equilibrium GDR  $\gamma$  emission, such as its dependences on impact parameter, isospin, EOS, etc.

So far both experimental data and theoretical calcula-

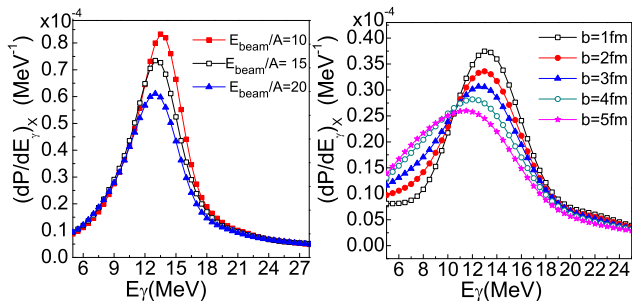


FIG. 3: (Color online) Left: Dipole dynamical emission spectra of the  $^{40}\text{Ca}+^{48}\text{Ca}$  system at 10, 15, and 20 MeV/nucleon, with impact parameters  $b = 1$  fm and soft EOS parameters. Right: Dynamical dipole  $\gamma$ -ray yield distribution of the  $^{40}\text{Ca}+^{48}\text{Ca}$  system at 10 MeV/nucleon in the early 400 fm/c, with impact parameter  $b$  varied from 1 to 5 fm and soft EOS parameters.

tions have shown that both the centroid and the width of the pre-equilibrium dipole component, with the exception of the  $\gamma$ -ray yield of GDR, are almost independent of the beam energy, and in this study, a similar conclusion was drawn from the left panel in Fig. 3, where we report calculations of the dynamical  $\gamma$ -ray emission of  $^{40}\text{Ca}+^{48}\text{Ca}$  at  $E_{\text{beam}} = 10, 15,$  and  $20$  MeV/nucleon, respectively. In the figure, the centroid and width of  $\gamma$  spectra seem insensitive to the incident energy, but the  $\gamma$ -ray emission probability  $dP/dE$  is suppressed at higher incident energies. A direct reduction of the initial charge asymmetry owing to pre-equilibrium nucleon emission (mostly neutrons) may account for the depressed  $\gamma$  yield. In addition, a higher excitation energy deposited in the composite system can damp the GDR emission. The suppressed behavior of  $\gamma$ -ray emission with increasing incident energy means that the heavy-ion collisions at a relative low energy are suitable for studying the collective dipole resonance. In fact, the conclusion here was supported by the existence of the dynamical dipole mode studied in fusion [15–17] and deep-inelastic heavy-ion collisions [10, 15].

The right panel in Fig. 3 gives the  $\gamma$ -ray emission probability of the  $^{40}\text{Ca}+^{48}\text{Ca}$  system at 10 MeV/nucleon on a scale of 0–400 fm/c, with  $b = 1$ –5 fm and soft EOS parameters. Both the yield and the central energy of the  $\gamma$ -ray distribution show a decreasing tendency with a larger impact parameter. As we know, a larger impact parameter inevitably induces a larger time scale of the isospin variation, corresponding to a low frequency of the dipole resonance, and thus leads to a lower central energy. Besides, collisions with different impact parameters, corresponding to different angular momenta, may generate dinuclei of different geometrical shapes [18], and necessarily, a larger impact parameter produces a dinuclei system with a larger deformation. Using the conclusion in Ref.[17], the GDR in a deformable CN is expected to have a central energy lower than that in a spherical nucleus of similar mass. Therefore the suppression of the central energy with an increasing impact parameter can also be partly attributed to the larger deformation of the dinuclei at the emission moment. What is more, the de-

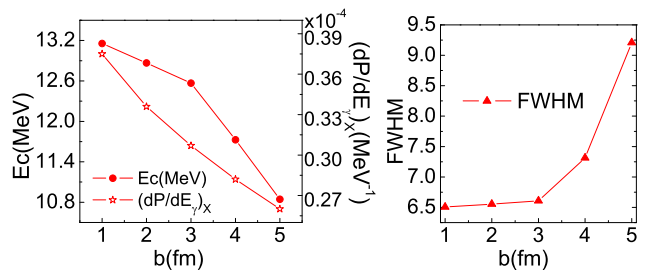


FIG. 4: (Color online) Left: Central energy  $E_c$  of the system  $^{40}\text{Ca}+^{48}\text{Ca}$  and corresponding maximum  $\gamma$ -emission probability  $(dP/dE_\gamma)_x$  as a function of  $b$  with  $E_{\text{beam}} = 10$  MeV/nucleon and soft EOS parameters. Right: Corresponding variation of the pre-equilibrium GDR width of the system.

formation of the CN may also bring about an anisotropic angular distribution pattern of the  $\gamma$  ray, which implies that investigation of the anisotropic angular distribution of GDR emission may also be a promising way to obtain information on the deformation of the composite system, which deserves further investigation.

Dependences of the centroids of pre-equilibrium GDR  $\gamma$ -ray spectra and maximum yields on the impact parameter are plotted in the left panel in Fig. 4; both the central energy (i.e., peak energy, denoted  $E_c$ ) and the corresponding maximum  $\gamma$ -ray yield,  $(dP/dE_\gamma)_x$ , decrease monotonously with increasing impact parameter. Meanwhile, the slower isospin equilibration process for a large impact parameter may enhance the emission of low-energy and multicomponent  $\gamma$  rays, and this could explain why the dynamical dipole emission width (denoted FWHM) increases with the impact parameter, which is shown in the right panel in Fig.4.

The sensitivity of the  $\gamma$ -ray yield to the stiffness of the EOS is also studied by comparing the simulation with soft and stiff Skyrme potentials. The evolution of a giant dipole moment for the  $^{40}\text{Ca}+^{48}\text{Ca}$  system, at  $E_{\text{beam}} = 10$  MeV/nucleon and  $b = 4$  fm, with different EOS parameters, soft EOS (filled circles) and stiff EOS (open stars), are plotted in the left panel in Fig.5; the corresponding  $\gamma$ -emission probability of the system, in the right panel. As shown in the figure, the stiff Skyrme potential generally leads to larger centroid and stronger dynamical dipole  $\gamma$  ray than the soft one.

Furthermore, the correlation between the dynamical dipole emission and the symmetry term of the EOS is also investigated by changing the symmetry energy coefficient ( $C_{\text{sym}}$ ). In the left panel in Fig.6, the spectrum of dynamical emission of the same system is reported, and the calculation is performed in the same situation except for the  $C_{\text{sym}}$ . We can clearly see an increased yield of  $\gamma$  rays for larger  $C_{\text{sym}}$  values.

As mentioned before, another interesting aspect of the GDR emission property is its dependence on the  $N/Z$  asymmetry of the reaction systems, which in fact is a direct result of Eq.(6). This relationship, indeed, is of most importance for its association with the symmetry term of the EOS. Presently, taking the charge and

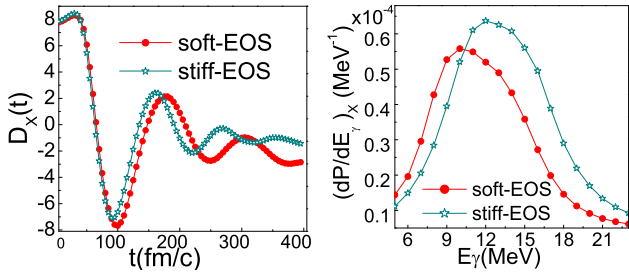


FIG. 5: (Color online) Left: The giant dipole moment evolves with time for the  $^{40}\text{Ca}+^{48}\text{Ca}$  system at  $E_{\text{beam}} = 10$  MeV/nucleon and  $b = 4$  fm; Right: The corresponding  $\gamma$ -emission probability of the system. Symbols are defined in the keys.

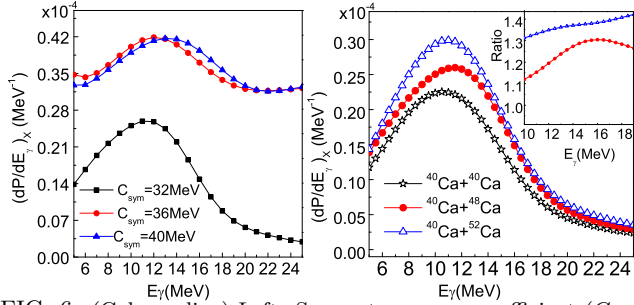


FIG. 6: (Color online) Left: Symmetry energy coefficient ( $C_{\text{sym}}$ ) dependence of  $\gamma$ -emission probability for the system  $^{40}\text{Ca}+^{48}\text{Ca}$  at  $E_{\text{beam}} = 10$  MeV/nucleon and  $b = 4$  fm. Right:  $\gamma$ -emission probability of systems  $^{40}\text{Ca}+^{52}\text{Ca}$ ,  $^{40}\text{Ca}+^{48}\text{Ca}$  and reference system  $^{40}\text{Ca}+^{40}\text{Ca}$  at  $E_{\text{beam}} = 10$  MeV/nucleon and  $b = 4$  fm with soft EOS ( $C_{\text{sym}} = 32$  MeV). Inset: Ratio of  $\gamma$  yields of systems with a  $^{48}\text{Ca}$  target or  $^{52}\text{Ca}$  target to those with a  $^{40}\text{Ca}$  target. Symbols are defined in the keys.

mass symmetric system  $^{40}\text{Ca}+^{40}\text{Ca}$  as a reference system, whose pre-equilibrium effect is not expected because of small initial dipole moment, we performed calculations of dipole  $\gamma$  emission in  $N/Z$  asymmetry systems, namely,  $^{40}\text{Ca}+^{48}\text{Ca}$  and  $^{40}\text{Ca}+^{52}\text{Ca}$ . In the right panel in Fig. 6, we show our results for  $\gamma$  emission in the early 400 fm/c at  $E_{\text{beam}} = 10$  MeV/nucleon, with  $b = 4$  fm and soft EOS. In the inset, the ratios of  $\gamma$  yields are also shown, where the ratio between the  $^{40}\text{Ca}+^{48}\text{Ca}$  and the  $^{40}\text{Ca}+^{40}\text{Ca}$  systems is shown by filled circles and the ratio between the  $^{40}\text{Ca}+^{52}\text{Ca}$  and the  $^{40}\text{Ca}+^{40}\text{Ca}$  systems is

denoted by open triangles. From the figure, we find that the  $N/Z$  asymmetry systems  $^{40}\text{Ca}+^{52}\text{Ca}$  ( $N/Z = 1.3$ ) and  $^{40}\text{Ca}+^{48}\text{Ca}$  ( $N/Z = 1.2$ ) show a clear enhanced yield of the order of about 35% and 20%, with respect to the symmetry system  $^{40}\text{Ca}+^{40}\text{Ca}$  ( $N/Z = 1.0$ ), consistent with results in Ref.[4] and references therein.

Experimental observations in Refs.[19] and [20] demonstrated that statistical  $\gamma$  emission is insensitive to a particular reaction entrance channel when we select the same phase-space region of the initial CN. Therefore, the evidenced extra  $\gamma$  yield can be explained by the dynamics of the compound system formed by a target and projectile with a large  $N/Z$  asymmetry. In contrast, the equilibrium GDR width and the peak energy are rather insensitive to isospin asymmetry [21].

In summary, we have applied the QMD model to investigate pre-equilibrium giant dipole oscillations (the dynamical dipole) and made systematical calculations for the low-energy reactions of  $^{40}\text{Ca}+\text{Ca}$  isotopes. The results show that dynamical dipole  $\gamma$  radiation is a good probe for gathering important information on the early stage of fusion, in particular, the charge asymmetry entrance channel. The dependences of the beam energy and impact parameter of the dipole resonance are discussed. The extra yield of pre-equilibrium GDR emission for systems with a large  $N/Z$  asymmetry suggests a strong dependence of dynamical emission on isospin asymmetry of the CN or, in other words, on the symmetry term of the EOS of nuclear matter. Meanwhile, the sensitivities of dynamical spectrum properties to the mean field potential and its symmetry energy portion indicate that detailed study of dynamical dipole  $\gamma$  radiation can be used as a probe to study the EOS around the normal nuclear density.

This work was supported in part by the National Natural Science Foundation of China under Contract Nos. 10775167, 10979074, 10875167, and 10747163, the Major State Basic Research Development Program in China under Contract No. 2007CB815004, the Chinese Academy of Science Foundation under Grant No. CXJJ-216 and the Shanghai Development Foundation for Science and Technology under Contract No. 09JC1416800.

- 
- [1] H. Hofmann et al., Z. Phys. A **293**, 229 (1979).  
[2] M. Di Toro, C. Gregoire, Z. Phys. A **320**, 321 (1985).  
[3] K. A. Snover, Annu. Rev. Nucl. Part. Sci. **36**, 545 (1986).  
[4] M. Papa et al., Phys. Rev. C **68**, 034606 (2003).  
[5] C. Simenel, P.Chomaz, and G.deFrance, Phys. Rev. Lett. **86**, 2971 (2001).  
[6] M. Di Toro et al., Int. J.Mod. Phys. E **17**, 110 (2008).  
[7] A. Corsi et al., Phys. Lett. B **679**, 197 (2009).  
[8] V. Baran et al., Phys. Rep. **410**, 335 (2005); B. A. Li et al., Phys. Rep. **464**, 113 (2008) and references therein.  
[9] V. Baran, C. Rizzo, M. Colonna, M. DiToro, and D. Pierroutsakou, Phys. Rev. C **79**, 021603(R) (2009).  
[10] M. Papa et al., Phys. Rev. C **72**, 064608 (2005).  
[11] J. Aichelin, Phys. Rep. **202**, 233 (1991).  
[12] Y. G. Ma et al, Phys. Rev. C **73**, 014604 (2006).  
[13] W. D. Tian et al., Chin. Phys. Lett. **22**, 306 (2005).  
[14] V. Baran et al, Nucl. Phys. A **679**, 373 (2001).  
[15] F. Amorini et al., Phys. Rev. C **69**, 014608 (2004).  
[16] S. Flibotte et al., Phys. Rev. Lett. **77**, 1448 (1996).  
[17] D. Pierroutsakou et al., Eur. Phys. J. A **17**, 71 (2003); Phys. Rev. C **71**, 054605 (2005); Phys. Rev. C **80**, 024612 (2009).  
[18] A. Bracco et al., Phys. Rev. Lett. **74**, 3748 (1995)  
[19] M. Thoennessen et al., Phys. Rev. Lett. **70**, 4055 (1993).

- [20] K.R. Sreenivasan, S.I. Vainshtein, R. Bhiladvala, I. SanGil, S. Chen, and N. Cao, Phys. Rev. Lett. **77**, 1488 (1996).
- [21] J. S. Wang et al., Eur. Phys. J. A **7**, 355 (2000).